



## Site-directed mutagenesis of human cytosolic sulfotransferase (SULT) 2B1b to phospho-mimetic Ser348Asp results in an isoform with increased catalytic activity

Emily D. Salman<sup>a</sup>, Dongning He<sup>a</sup>, Melissa Runge-Morris<sup>b</sup>, Thomas A. Kocarek<sup>b</sup>, Charles N. Falany<sup>a,\*</sup>

<sup>a</sup> Department of Pharmacology and Toxicology, University of Alabama at Birmingham, Birmingham, AL 35294, United States

<sup>b</sup> Institute of Environmental Health Sciences, Wayne State University, Detroit, MI 48201, United States

### ARTICLE INFO

#### Article history:

Received 12 May 2011

Received in revised form 29 June 2011

Accepted 26 July 2011

#### Keywords:

Sulfotransferase

Hydroxysteroid

Nuclear translocation

Phosphorylation

Cholesterol

Metabolism

Dehydroepiandrosterone

### ABSTRACT

Human SULT2B1b is distinct from other SULT isoforms due to the presence of unique amino (N)- and carboxy (C)-terminal peptides. Using site-directed mutagenesis, it was determined that phosphorylation of Ser348 was associated with nuclear localization. To investigate the effects of this phosphorylation of Ser348 on activity and cellular localization, an *in silico* molecular mimic was generated by mutating Ser348 to an Asp. The Asp residue mimics the shape and charge of a phospho-Ser and homology models of SULT2B1b-phospho-S348 and SULT2B1b-S348D suggest a similar significant structural rearrangement in the C-terminal peptide. To evaluate the functional consequences of this post-translational modification and predicted rearrangement, 6His-SULT2B1b-S348D was synthesized, expressed, purified and characterized. The 6His-SULT2B1b-S348D has a specific activity for DHEA sulfation ten-fold higher than recombinant 6His-SULT2B1b (209.6 and 21.8 pmol min<sup>-1</sup> mg<sup>-1</sup>, respectively). Similar to native SULT2B1b, gel filtration chromatography showed SULT2B1b-S348D was enzymatically active as a homodimer. Stability assays comparing SULT2B1b and SULT2B1b-S348D demonstrated that SULT2B1b is 60% less thermostable than SULT2B1b-S348D. The increased stability and sulfation activity allowed for better characterization of the sulfation kinetics for putative substrates as well as the determination of dissociation constants that were difficult to obtain with wild-type (WT) 6His-SULT2B1b. The  $K_D$ s for DHEA and PAPS binding to 6His-SULT2B1b-S348D were  $650 \pm 7$  nM and  $265 \pm 4$  nM, respectively, whereas  $K_D$ s for binding of substrates to the WT enzyme could not be determined. Characterization of the molecular mimic SULT2B1b-S348D provides a better understanding for the role of the unique structure of SULT2B1b and its effect on sulfation activity, and has allowed for improved kinetic characterization of the SULT2B1b enzyme.

© 2011 Elsevier Ltd. All rights reserved.

### 1. Introduction

Human cytosolic sulfotransferases (SULT) are a family of Phase II drug-metabolizing enzymes that conjugate a sulfonate (SO<sub>3</sub><sup>-</sup>) group from the obligate sulfonate donor 3'-phosphoadenosine 5'-phosphosulfate (PAPS) to an acceptor hydroxyl or amine group [1]. The two families of human SULTs that have been best characterized are designated SULT1 and SULT2 [1]. The SULT1 isoforms catalyze the sulfation of small phenols such as naphthols, estrogens, dietary polyphenols and catecholamines [2–4]. The SULT2 isoforms conjugate hydroxysteroids such as dehydroepiandrosterone (DHEA), cholesterol, bile acids and pregnenolone [5–8]. There are also isoforms in humans designated SULT4A1 (Br-STL)

and SULT6B1; however, there are no known substrates for these enzymes [9,10].

SULT2A1 and SULT2B1b are the major isoforms in the human SULT2 family [11]. The SULT2B1 gene encodes two transcripts for the isoforms, SULT2B1a or SULT2B1b, which differ by 8 amino acids due to the use of alternate transcriptional start sites. However, to date only SULT2B1b protein has been detected in any human tissue or cell line investigated [12]. SULT2A1 is primarily expressed in liver and adrenal glands [13,14], while SULT2B1b is expressed in the lungs, skin, brain, breast, endometrium, gastrointestinal tract and prostate [15–17]. SULT2A1 is capable of sulfonating 3- and 17-hydroxysteroids, bile acids and estrogens, while SULT2B1b is selective for the conjugation of 3β-hydroxysteroids [11,18]. Another characteristic that distinguishes SULT2B1b from the other human SULT isoforms is the presence of a 16- amino acid amino-terminal (N-) extension and a 45-amino acid carboxy-terminal (C-) extension [19]. Further, SULT2B1b is the only SULT isoform known to show nuclear translocation and post-translational modification [19]. While the reaction mechanisms, substrate-specificity,

\* Corresponding author at: 1670 University Blvd, VH 151, Birmingham, AL 35294, United States. Tel.: +1 205 934 9848; fax: +1 205 934 8240.

E-mail address: [cfalany@uab.edu](mailto:cfalany@uab.edu) (C.N. Falany).

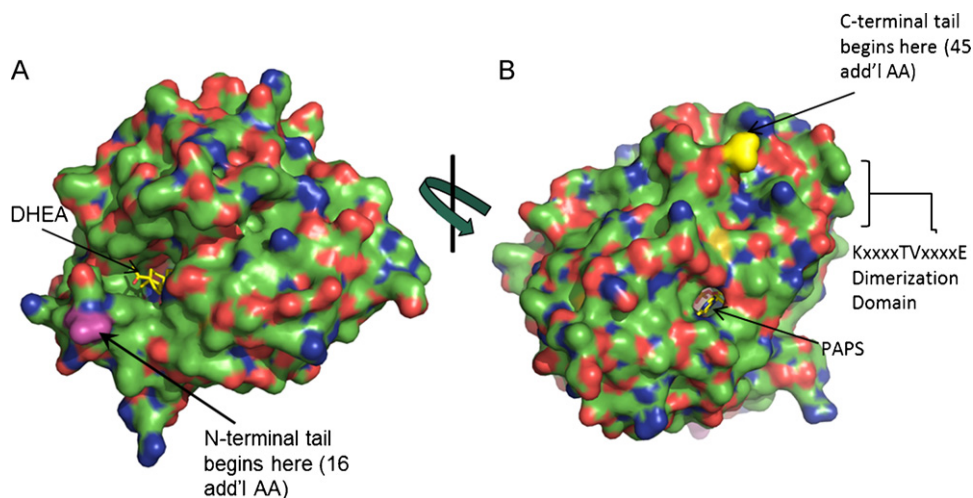


**Fig. 1.** Crystal structures for SULT2B1b lack N- and C-terminal peptide extensions. The crystal structure for SULT2B1b (1Q22) was crystallized in the presence of DHEA and PAP. Due to the dynamic nature of the N- and C-terminal peptides, the peptides failed to resolve in the crystal structures. Shown in magenta with large arrow (A) is the site at which the 16 additional amino acids of the N-terminus would join the core of the enzyme. The substrate binding pocket is marked by the small arrow, shown with DHEA bound in yellow. In B, the crystal structure is rotated to show the opposite face of the enzyme. Shown in yellow with large arrow is the site at which the 45 additional amino acids of the C-terminal extension would join the core of the enzyme. (For interpretation of the references to color in this figure legend, the reader is referred to the web version of the article.) The PAPS binding pocket is marked by the small arrow, with PAP shown in yellow.

and tissue distribution of SULT isoforms have been the subject of many investigations, little is understood about the role of post-translational modification in the regulation or function of the SULTs.

Our laboratory has described the cloning, expression and purification of human SULT2B1b and has investigated extrahepatic tissue-specific expression patterns of this isoform. SULT2B1b shows both cytosolic and nuclear expression in breast and placental cell types, although the ratio of cytosolic to nuclear expression varies in these cells [16,17,20,21]. SULT2B1b protein is found almost exclusively in the nuclei of term placenta, while nuclear expression varies significantly in normal breast and breast cancer specimens [21]. In other tissues, such as brain and prostate, SULT2B1b is expressed in the cytosol and is apparently not localized in the nuclei [16].

The N- and C-terminal peptides are unique characteristics of the SULT2B1 isoforms; however, both the N- and C-terminal peptides failed to resolve in the published crystal structures for SULT2B1a (PDB no. 1Q1Q) and SULT2B1b (PDB no. 1Q1Z, 1Q20, and 1Q22) [22]. Therefore, the crystal structures do not provide insight into the structure or functional consequences of the N- and C-terminal extensions of the enzyme. The substrate binding site, PAPS binding site and putative dimerization domain (KxxxTVxxxE) are in close proximity to the location at which the N- and C-terminal extensions join the core of the enzyme (Fig. 1). For this reason, it is important to investigate the relationship between the peptide extensions of SULT2B1b and the core of the enzyme and the effect the extensions may have on enzymatic function. Truncation and mutagenesis experiments by Fuda et al. [23] performed on the N-terminus of the enzyme have shown that residues on the N-terminus confer some degree of substrate specificity to the enzyme; however, there have been no reports of the structural or functional consequences of the C-terminus of SULT2B1b, other than that the peptide is essential for enzymatic activity [19].

Phosphorylation of the C-terminal peptide of SULT2B1b was first described in 2006 by where it was shown that a phosphorylation event contributes to the nuclear translocation in human BeWo choriocarcinoma cells [19]. The C-terminus of SULT2B1b is serine- and proline-rich with many potential sites for phosphorylation and post-translational modification. Mass spectrometric analysis revealed that the phosphorylation event for stably expressed

SULT2B1b in BeWo cells occurred on a peptide fragment corresponding to residues 341–365 [19]. Since the kinase responsible for this post-translational modification is unknown, a phospho-mimetic was generated by mutating the serine associated with phosphorylation to an aspartate (Asp) residue to mimic the shape and charge of a phospho-serine residue. Several studies have utilized phospho-mimetic constructs of proteins to elucidate the biochemical and physiological consequences of phosphorylation, including prolactin, pregnane-X-receptor [24], focal adhesion kinase [25], and casein kinase I [26].

In order to identify the mechanism of nuclear localization, the consequences of SULT2B1b phosphorylation, and to elucidate the site of phosphorylation, serine (Ser) residues in the 341–365 peptide were individually mutated, and the mutated proteins were expressed and characterized for sub-cellular localization. Molecular modeling and in silico mutagenesis were performed to better understand the structural consequences that phosphorylation of Ser residues may have on SULT2B1b. Mutagenesis, expression, and purification of a molecular mimic of phospho-SULT2B1b and characterization of its sulfation activity could increase our understanding of this unique SULT isoform as well as provide a biochemical tool for exploring the nuclear localization of SULT2B1b.

## 2. Materials and methods

### 2.1. Materials

Oligonucleotide primers were synthesized by Operon (Huntsville, AL). [<sup>3</sup>H]-DHEA (79 Ci/mmol), and [<sup>3</sup>H]-pregnenolone (25 Ci/mmol) were purchased from Perkin-Elmer (Boston, MA). Non-radiolabeled PAPS was obtained from Dr. Sanford Singer (University of Dayton, OH). Mouse anti-histone monoclonal IgG was purchased from Millipore (Billerica, MA). Affinity-purified goat anti-rabbit and anti-mouse horseradish peroxidase conjugated IgG were purchased from Southern Biotechnology (Birmingham, AL). The Super Signal chemiluminescence substrate kit and Mammalian Protein Extraction Reagent (MPER) were purchased from Thermo Fisher (Rockford, IL). Platinum Taq DNA Polymerase, pCDNA3.1, Lipofectin, and pProExHTa were purchased from Invitrogen (Carlsbad, CA). QuickChange II XL Site-Directed Mutagenesis Kit and *Pfu* Polymerase were purchased from Agilent Technologies

(Santa Clara, CA). OptiPrep media, size-exclusion molecular weight standards, adenosine 3',5'-diphosphate sodium (PAP), geneticin, and Ni-NTA resin were purchased from Sigma (St. Louis, MO). BeWo cells were obtained from ATTC (Manassas, VA). All other chemicals were of reagent grade quality.

## 2.2. Determination of key serine residues involved in phosphorylation of SULT2B1b

The full-length SULT2B1b open reading frame was amplified by PCR *Pfu* polymerase using forward primer 5'-GATTCGAATTCGGCATGGACGGG-3', to incorporate an *EcoR* I site and reverse primer 5'-GACGGTCAAGCTTATTATGAGGGTCGTGGG-3', to incorporate a *Hind* III site. The amplified SULT2B1b cDNA was restriction digested, purified and ligated into the mammalian expression vector pcDNA3.1.

Site-directed mutagenesis was performed by PCR using Platinum Taq DNA Polymerase according to the procedure of the QuickChange II XL Site-Directed Mutagenesis Kit. Using the SULT2B1b plasmid as a template, the codon encoding Ser347 was mutated to GCC to create an Ala and the codons encoding Ser348, Ser352 and Ser357 were mutated to GGG to yield Gly residues. Ser347 was mutated to an Ala rather than a Gly due to codon usage in the SULT2B1b mRNA sequence, and to avoid changing more than 2 nucleotides at a time. The pcDNA3.1/SULT2B1b WT and mutant plasmids were transfected into BeWo human placental choriocarcinoma cells using Lipofectin at a DNA/Lipofectin ratio of 1:3 in Opti-MEM followed by selection with 400 µg/ml geneticin until geneticin-resistant colonies formed. Cytosol, microsomes and nuclei were isolated from transfected BeWo cells using differential centrifugation with an OptiPrep gradient. SULT2B1b was identified in the isolated fractions by immunoblot analysis with rabbit anti-SULT2B1b IgG [11]. Nuclei were identified by immunoblot analysis with a mouse anti-histone monoclonal antibody.

## 2.3. Molecular modeling

In silico models for SULT2B1b and mutants were constructed using the platform *Molecular Operating Environment* (MOE) (Ver. 2009.10) from the Chemical Computing Group, Inc. (Montreal, Quebec, Canada). The N- and C-terminal peptide extensions of SULT2B1b fail to resolve during crystallography of the enzyme; therefore, all three published crystal structures for SULT2B1b lack the resolution of N- and C-terminal extensions [22]. A homology model was constructed to represent the full-length SULT2B1b and to provide a template for performing in silico mutagenesis. N- and C- peptides were constructed using the Builder function in MOE and energy minimization of these peptides was performed using the AMBER99 algorithm. The peptides were attached to the body of SULT2B1b and the entire amino acid sequence was threaded onto the previously published SULT2B1b crystal structure 1Q22, which was selected since the enzyme was crystallized in the presence of pregnenolone and PAP. The homology model was generated using the Homology Model function in MOE and the top 5 ranked structures were checked for errors using the NIH Structural Analysis and Verification Server (SAVES) database [27–29]. Phosphoserine348 and Asp348 mutations were created using the mutate function in MOE and energy minimizations performed. Docking experiments were performed using known substrates to ensure proper binding of these structures into the active site of the enzyme as well as to determine whether putative substrates for SULT2B1b could dock into the active site of the enzyme. Substrates were oriented in the active site of SULT2B1b (1Q22) with Triangle matcher using the AMBER99 force field to perform energy minimizations using DHEA as a template in the substrate binding pocket. Refinements were carried out using an Affinity dG algorithm to perform the scoring of

the different structures. The top five structures with the lowest BFE from each substrate-enzyme combination of the docking studies were evaluated.

## 2.4. Generation of SULT2B1b-S348D mutant

Mutagenesis of SULT2B1b was performed using the QuickChange II XL Site-Directed Mutagenesis Kit. Oligonucleotide primers were designed to mutate Ser348 to Asp. Briefly, SULT2B1b in the bacterial expression vector pProExHTa was used as the template for the mutagenesis PCR where 2.5 U *PfuUltra* high-fidelity DNA polymerase was used to amplify SULT2B1b using the following cycling parameters: 95 °C for 1 min, then 18 cycles of 95 °C for 50 s, 60 °C for 50 s, and 68 °C for 6 min, followed by 68 °C for 7 min. After PCR amplification, restriction endonuclease *Dpn* I was added and the reactions were incubated at 37 °C for 1 h in order to digest any remaining parental DNA. Digested amplicons were then used in transformation reactions with chemically competent *E. coli* XL10-Gold Ultracompetent cells [6]. Plasmid DNA was purified from overnight cultures, and quantified by UV spectroscopy, and the presence of the mutation was confirmed by sequence analysis.

## 2.5. Enzyme expression and protein purification

Recombinant 6HisSULT2B1b and 6HisSULT2B1b-S348D protein expression was induced as described previously [11]. Briefly, bacterial expression of 6HisSULT2B1b and 6HisSULT2B1b-S348D was induced with 0.3 mM isopropyl-β-D-thiogalactopyranoside (IPTG) for 2 h. The bacterial pellet was recovered by centrifugation at 1500 × g for 30 min then the pellet was resuspended at 2 ml g<sup>-1</sup> of column buffer (20 mM Tris-HCl, 100 mM KCl, 5 mM 2-mercaptoethanol, 10% glycerol, pH 8.5 at 4 °C) and lysed by sonication. Cytosol was prepared from crude cell lysates by ultracentrifugation at 100,000 × g at 4 °C for 45 min. 6His-SULT2B1b and 6His-SULT2B1b-S348D were purified from the bacterial cytosol using Ni-NTA affinity chromatography. Fractions containing the highest SULT2B1b activity were pooled and dialyzed overnight in column buffer to remove imidazole.

## 2.6. Size exclusion chromatography

A 45 cm × 1 cm G-75 Sephadex column was equilibrated in column buffer at 4 °C. The gel filtration column was standardized using bovine serum albumin (MW 66 kDa), bovine hemoglobin (MW 64.5 kDa), cytochrome c (MW 12 kDa), and equine carbonic anhydrase (MW 31 kDa) and determining the absorbance at 590 nm. Approximately 200 µg of either 6His-SULT2B1b or 6His-SULT2B1b-S348D was loaded onto the column and 1 ml fractions were collected and assayed for sulfation activity.

## 2.7. SULT assays

Sulfation activity for SULTB1b was quantified using a chloroform extraction assay described previously [30]. Briefly, 0–10 µM [<sup>3</sup>H]-DHEA or [<sup>3</sup>H]-pregnenolone was used in reactions with unlabeled PAPS (25 µM) and purified recombinant SULT2B1b in reaction buffer (50 mM Tris-HCl, pH 7.4, 1 mM MgCl<sub>2</sub>). Reactions were incubated at 37 °C for the desired time and stopped by addition of 3 ml CHCl<sub>3</sub> and alkalized with 375 µl 1.5 M Tris-HCl, pH 8.5. Reactions were vortexed, and centrifuged at 1000g, then an aliquot of the aqueous layer was counted in a liquid scintillation counter. All assays were performed in triplicate with no substrate and no PAPS reactions as controls. Sulfation activity is presented as pmol<sup>-1</sup> min<sup>-1</sup> mg<sup>-1</sup> ± SEM.

Sulfation activity with non-radiolabeled acceptor compounds was determined using [<sup>35</sup>S]-PAPS as described previously [6]. The

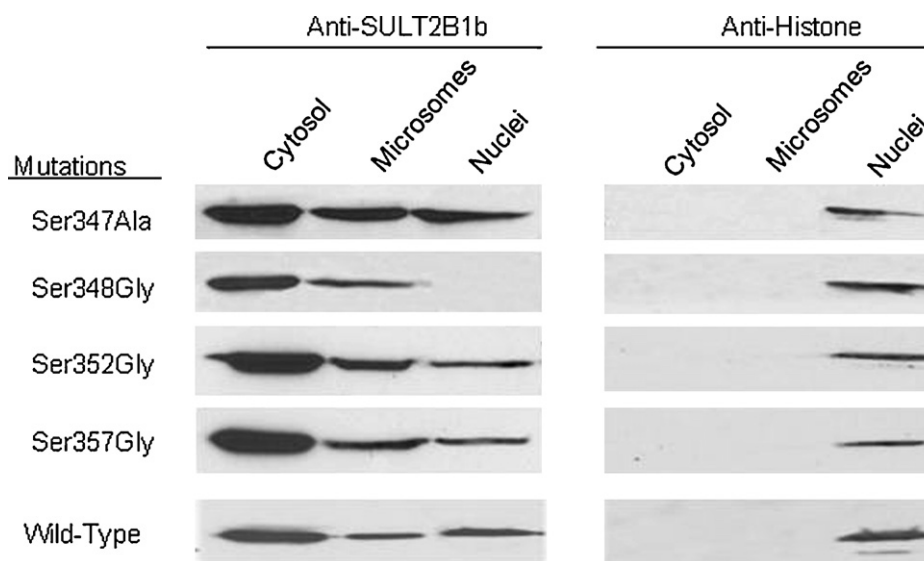


**Fig. 2.** Subcellular localization of WT and mutants of SULT2B1b in transfected BeWo cells. Cytosol, microsomes and nuclei were isolated from BeWo cells transformed with either WT pcDNA3.1/SULT2B1b, pcDNA3.1/SULT2B1b S347A, pcDNA3.1/SULT2B1b S348G, pcDNA3.1/SULT2B1b S350G, or pcDNA3.1/SULT2B1b S352G using an Optiprep gradient and differential centrifugation. Mutated residues were selected based on mass spectrometric analysis showing a phosphorylated Ser in peptide 341–363). Subcellular fractions on duplicate immunoblots were analyzed with either anti-SULT2B1b IgG (A) to evaluate subcellular localization of enzyme, or mouse anti-histone monoclonal antibody (B) to demonstrate the purity of the nuclear fractions.

reactions contained 50 mM Tris–HCl, pH 7.4, 1 mM MgCl<sub>2</sub>, 25 μM [<sup>35</sup>S]-PAPS, and 0–20 μM substrate in a final volume of 65 μl. Purified recombinant SULT2B1b-S348D was used to start reactions. Reactions were incubated for 15 min at 37 °C and terminated by spotting a 50 μl aliquot of each reaction onto a silica gel F-250 TLC plate. For oxysterols, the TLC plate was developed in methylene chloride/methanol/ammonium hydroxide (85:15:5, v/v/v). The [<sup>35</sup>S]-labeled products were localized by autoradiography and then scraped into scintillation vials for determination of radioactivity by liquid scintillation spectroscopy. All assays were performed in triplicate, and no substrate reactions were used as controls.

### 2.8. Immunoblot analysis

Samples (100–200 μg total protein) were electrophoresed in 10% SDS/polyacrylamide gels at 200V for approximately 40 min. Gels were equilibrated in semi-dry transfer buffer (48 mM Tris, 39 mM glycine, 20% methanol, pH 9.2) for 15 min prior to transfer of resolved proteins to nitrocellulose membranes at 12 V for 35 min in a BioRad Semi-dry Transfer Unit. Membranes were blocked in 5% non-fat milk in Tris-buffered saline (TBS, pH 7.4) for 1 h prior to incubation with primary antibody. For SULT2B1b immunoblot analysis, membranes are incubated in rabbit anti-SULT2B1 IgG, diluted 1:1000 in 0.1% non-fat milk in TBS, for 1 h. This antibody has been made and validated by our laboratory [11]. After incubation with primary antibody, immunoblots were incubated in goat anti-rabbit horseradish peroxidase (1:50,000) and developed in Super Signal West Pico before exposing to autoradiograph film.

### 2.9. *K<sub>D</sub>* determinations for DHEA and PAP with SULT2B1b-S348D

Intrinsic fluorescence (IF) spectroscopy was used to evaluate binding constants of substrates binding to SULT2B1b. IF experiments were performed using a Perkin Elmer LS-5 luminescence spectrometer with a xenon source. Pilot experiments determined the optimal excitation wavelength as 278 nm, and an emission wavelength of 325 nm for SULT2B1b enzyme preparations (data not shown). For substrate binding studies, SULT2B1b preparations were diluted in phosphate-buffered saline (PBS, pH 7.4) to a final

concentration of 50 nM in 4-sided IF cuvettes with a 10 mm light path. Substrates were added in 1 μl increments and the enzyme mixture was allowed to equilibrate for 3 min after each addition and mixing by trituration. Titrations of substrates did not exceed a 5% increase in total volume. PAP was used instead of PAPS in the binding studies to avoid *in vitro* sulfonation activity. Relative fluorescence was recorded after each addition of substrate, with substrate binding expressed as change in relative fluorescence ( $I/I_0$ ).

## 3. Results

### 3.1. Identification of key serine residues in nuclear localization

Our laboratory previously reported that phosphorylation of the C-terminus of SULT2B1b is associated with nuclear localization [19]. In order to understand the mechanism for nuclear localization in SULT2B1b, the site of phosphorylation in the C-terminus SULT2B1b was determined. Mass spectrometric analysis of SULT2B1b indicated that a phosphorylation event occurred in peptide fragment 341–365 [19]. Ser residues (347, 348, 352, and 357) in this peptide were mutated to small, less reactive Ala or Gly residues using the pcDNA3.1/SULT2B1b expression vector as a template. WT and mutant pcDNA3.1/SULT2B1b constructs were transfected into BeWo cells and evaluated for subcellular localization [19]. Fig. 2 shows that immunoblot analysis of SULT2B1b in sub-cellular fractions of the transfected BeWo cells indicates that nuclear localization of SULT2B1b was lost when Ser348 was mutated to a Gly residue. Mutation of Ser347, Ser352 and Ser357 showed no change in sub-cellular localization.

### 3.2. Homology modeling and *in silico* mutagenesis

Since S348 appears to be required for nuclear localization, *in silico* molecular models of SULT2B1b phospho-S348 and the molecular mimic SULT2B1b-S348D were generated to evaluate the structural consequences of S348 phosphorylation. Because S348 is contained within the C-terminal peptide that failed to resolve following crystallization, a homology model of full-length SULT2B1b

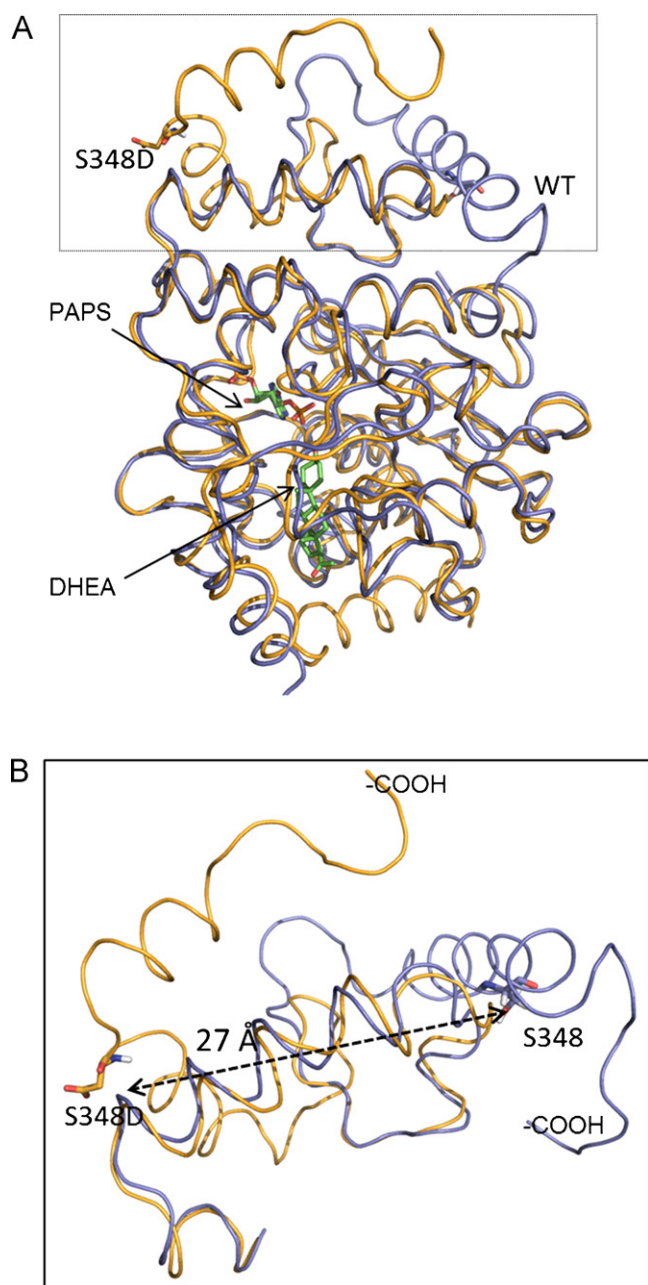


**Fig. 3.** Molecular models of Ser348Asp mutant mimicking phosphoserine in vivo. The molecular model for SULT2B1b-phosphoS348 was identical to the molecular model for SULT2B1b-S348D. Shown in panel A are the homology models of SULT2B1b (blue) and SULT2B1b-S348D (yellow). (For interpretation of the references to color in this figure legend, the reader is referred to the web version of the article.) Molecular models were constructed from energy minimization of the SULT2B1b peptide sequence using the SULT2B1b and SULT2A1 crystal structures (1Q22, 1EFH) as templates. The carboxy-terminal extension of SULT2B1b (blue) and SULT2B1b-S348D (yellow) are shown in panel B and illustrate the change in structure associated with the molecular mimic. The 27 Å shift in the position of S348 was measured using Pymol (Ver. 1.4).

was constructed (Fig. 3). In silico mutagenesis of SULT2B1b to SULT2B1b phospho-S348 and SULT2B1b-S348D was performed to predict if phosphorylation could have a structural effect on the enzyme and whether the predicted rearrangement would be similar for both constructs. As shown in Fig. 3, the molecular models for SULT2B1b phospho-S348 and SULT2B1b-S348D were identical. In both models, phosphorylation of S348 and mutagenesis of S348 to an Asp residue resulted in a 27 Å structural shift in the C-terminal extension in the models of the enzyme (Fig. 3A). The predicted shift

**Table 1**  
Scoring values of substrates docked into SULT2B1b structures.

Structure	DHEA (kJ)	Pregnenolone (kJ)
WT crystal structure (1Q20)	−9.5	−9.1
WT homology model	−9.6	−9.3
Ser348Asp model	−9.6	−9.4

Molecular models for SULT2B1b enzyme constructs were utilized in docking experiments to determine the ability of substrates to access and docking into the substrate binding sites for SULT2B1b. Docking experiments were performed in MOE using Proxy Triangle and Affinity dG algorithms. BFE was used as the scoring function for these experiments. The top 5 ranked structures were checked for errors using NIH Structural Analysis and Verification Server (SAVES) database.

in the C-terminal peptide is shown in Fig. 3B. In order to ensure the integrity of the substrate binding site in these molecular models, docking experiments were performed with these models using the known substrates DHEA and pregnenolone. There were no changes in the predicted ability of DHEA or pregnenolone to bind in the active site of the resolved crystal structure (1Q22), the WT homology model, or the molecular mimic S348D mutant demonstrating that the molecular models did not result in major changes to the structure of the active site of the enzyme models (Table 1).

### 3.3. Kinetic characterization of 6His-SULT2B1b-S348D

After the S348D mutation was confirmed by sequence analysis, recombinant 6His-SULT2B1b-S348D was expressed and purified from XL10-Gold *E. coli* by Ni<sup>2+</sup>-affinity chromatography [11]. Upon purification, 6His-SULT2B1b-S348D showed significantly higher sulfation activity for both DHEA and pregnenolone than the 6His-SULT2B1b protein (Fig. 4). The specific activity for 6His-SULT2B1b-S348D was ten times higher for DHEA sulfation than that of 6His-SULT2B1b at 21.8 and 209.6 pmol min<sup>−1</sup> mg<sup>−1</sup>, respectively.

### 3.4. 6His-SULT2B1b is enzymatically active as a dimer

Since the KxxxTVxxxE dimerization domain of SULT2B1b is in close proximity (8–12 Å) to the C-terminal extension (Fig. 1), it was prudent to determine whether dimerization of the enzyme was affected by the predicted structural rearrangement in SULT2B1b-S348D. Size-exclusion chromatography was used to evaluate the effect of the S348D mutation of SULT2B1b dimerization. Fig. 5 shows that purified, active recombinant 6His-SULT2B1b-S348D eluted as a dimer. Immunoblot analysis of column fractions for

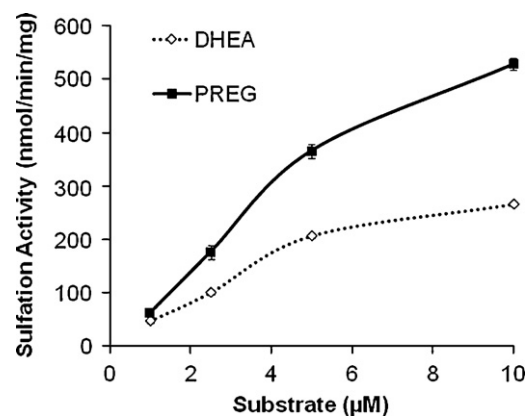


**Fig. 4.** Sulfation activity of bacterially-expressed purified recombinant 6His-SULT2B1b-S348D. Sulfation activity for 6His-SULT2B1b was determined by incubating 0.25 µg enzyme with 1–10 µM [<sup>3</sup>H]-DHEA or [<sup>3</sup>H]-pregnenolone, with PAPS (25 µM) for 10 min. No substrate and no PAPS were used as controls. Reactions were performed in triplicate, error bars represent SEM. Where not seen, error bars are contained within the data points.

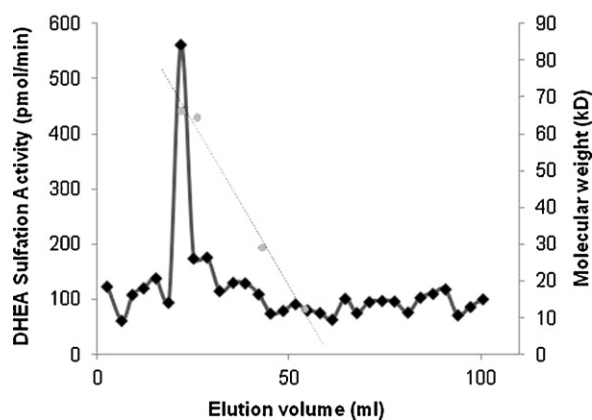


**Fig. 5.** Size-exclusion chromatography of bacterially-expressed recombinant human 6His-SULT2B1 S348D. Approximately 200 mg enzyme was loaded onto 45 cm × 1 cm G-75 Sephadex column. Eluent (25 μl) was assayed for sulfation activity in the presence of 10 μM [<sup>3</sup>H]-DHEA and 25 μM PAPS for 15 min. A peristaltic pump was used to maintain constant pressure and flow (1 ml·h<sup>-1</sup>) through the column. The gel filtration column was standardized using bovine serum albumin (MW 66 kDa), bovine hemoglobin (MW 64.5 kDa), cytochrome c (MW 12 kDa), and equine carbonic anhydrase (MW 31 kDa) and assaying absorbance of eluent (280 nm and 590 nm).

SULT2B1b correlated with enzyme activity (data not shown). Based upon calibration of the column with MW standards, there is no sulfation activity or immunoreactivity in fractions at which a monomeric SULT isoform would be anticipated to elute (data not shown).

### 3.5. Kinetic characterization and comparison of 6His-SULT2B1b and 6His-SULT2B1b S348D

To compare the sulfation activity of 6His-SULT2B1b and 6His-SULT2B1b-S348D, the recombinant enzymes were purified and used in DHEA and pregnenolone sulfation assays. Due to differences in the specific activity of the purified proteins, 2.5 μg 6His-SULT2B1b or 0.25 μg 6His-SULT2B1b-S348D was used in each reaction. Fig. 6 shows the DHEA sulfation kinetics for 6His-SULT2B1b and 6His-SULT2B1b-S348D. The  $K_m$  for DHEA is 10-fold lower for 6His-SULT2B1b-S348D than for 6His-SULT2B1b at 0.9 μM and 10.9 μM, respectively. The  $K_m$ s for pregnenolone are also 10-fold different, at 11.8 μM for 6His-SULT2B1b and 1.9 μM for

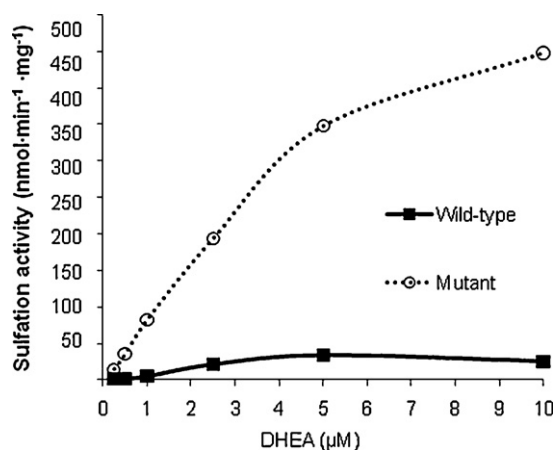


**Fig. 6.** Kinetic characterization and comparison of 6His-SULT2B1b and 6His-SULT2B1b S348D. Sulfation activity was determined using 0–10 μM [<sup>3</sup>H]-DHEA and 25 μM PAPS for 10 min. Due to differences in specific activity, 2.5 μg 6His-SULT2B1b or 0.25 μg 6His-SULT2B1b-S348D was used in each reaction. All reactions were performed in triplicate. Error bars represent SEM and are contained within the points.

**Table 2**

Apparent  $K_m$ s of DHEA, pregnenolone, and PAPS using SULT2B1b-expressed enzymes.

Enzyme Construct	DHEA (μM)	Pregnenolone (μM)	PAPS (μM)
6His-SULT2B1b	10.9 ± 0.1	11.8 ± 0.1	0.6 ± 0.10
6His-SULT2B1bS348D	0.9 ± 0.1	1.9 ± 0.07	0.8 ± 0.06

Expressed SULT2B1b isoforms with 6His-tags were used in extraction assays to determine the apparent  $K_m$ s of each construct for the substrates listed. DHEA and pregnenolone sulfation was assayed at concentrations between 0.5 μM and 20 μM using 25 μM PAPS. For the determination of apparent  $K_m$  for PAPS, assays were performed using 3 μM DHEA and PAPS concentrations between 0.25 μM and 25 μM. All assays were performed in triplicate,  $K_m$  values are expressed as ± SEM.

6His-SULT2B1b-S348D (Table 2). Ser348D mutagenesis had no effect on the  $K_m$  for PAPS (Table 2).

### 3.6. $K_D$ determination of substrates for SULT2B1b-S348D

The poor stability and sulfation activity of SULT2B1b made it difficult to determine dissociation constants ( $K_D$ ) for known substrates as the enzyme did not exhibit reproducible behavior in intrinsic fluorescence experiments. In contrast, the SULT2B1b-S348D mutant demonstrated significantly improved binding characteristics (Fig. 7). In order to determine the affinity of DHEA and PAPS for SULT2B1b-S348D, IF spectroscopy was used to determine the  $K_D$  values for the binding of these substrates to SULT2B1b-S348D. The  $K_D$  for DHEA binding to 6His-SULT2B1b-S348D was 650 ± 7 nM and 265 ± 2 nM for PAPS binding (Table 3). Our laboratory has reported that the  $K_D$ s for substrates binding to SULT2A1 are affected by the presence of the co-substrate [31]. In order to determine whether binding of substrate to SULT2B1b affected the ability of the second substrate to bind to SULT2B1b, the enzyme was incubated with either DHEA or PAP to saturate the respective binding site before performing the  $K_D$  experiments. In the presence of 5 μM PAP, the  $K_D$  for DHEA was 575 ± 2 nM. In the presence of 10 μM DHEA, the  $K_D$  for PAP was 278 ± 3 nM. There was no statistical difference between the  $K_D$ s in the presence or absence of co-substrate.

### 3.7. Stability assays for SULT2B1b and SULT2B1b-S348D

The sulfation activity of both recombinant SULT2B1b and cellular SULT2B1b is known to be highly unstable and active SULT2B1b has not been isolated from a human tissue [16,17]. Likewise, sulfation activity of SULT2B1b in intact cultured cells or nuclei cannot be detected once intact cells or nuclei have been lysed [16]. To compare the stability of SULT2B1b and the S348D mutant, DHEA sulfation assays were performed on 6His-SULT2B1b and 6His-SULT2B1b-S348D after incubation at 42 °C for 0–3 h. After 120 min, 6His-SULT2B1b retained only 20% of its original sulfation activity in contrast to 6His-SULT2B1b-S348D which retained 78% of its activity

**Table 3**

Dissociation constants ( $K_D$ ) for SULT2B1b substrates by intrinsic fluorescence spectroscopy.

Enzyme construct	Substrate	$K_D$ (nM)
6His-SULT2B1b S348D	DHEA	650 ± 7
6His-SULT2B1b S348D + PAP	DHEA	575 ± 8
6His-SULT2B1b S348D	PAP	265 ± 6
6His-SULT2B1b S348D + DHEA	PAP	278 ± 11

For substrate binding studies, SULT2B1b preparations were diluted in phosphate-buffered saline (pH 7.4) to a final concentration of 50 nM. Enzyme was allowed to equilibrate for 3 min after each addition of substrate in 1 μl increments, so as not to exceed a 5% increase in total volume, and mixed by trituration. PAP was used instead of PAPS in the binding studies to avoid in vitro sulfonation. Relative fluorescence was recorded after each addition of substrate, with substrate binding expressed as change in relative fluorescence. All experiments were performed in triplicate, error bars represent SEM.

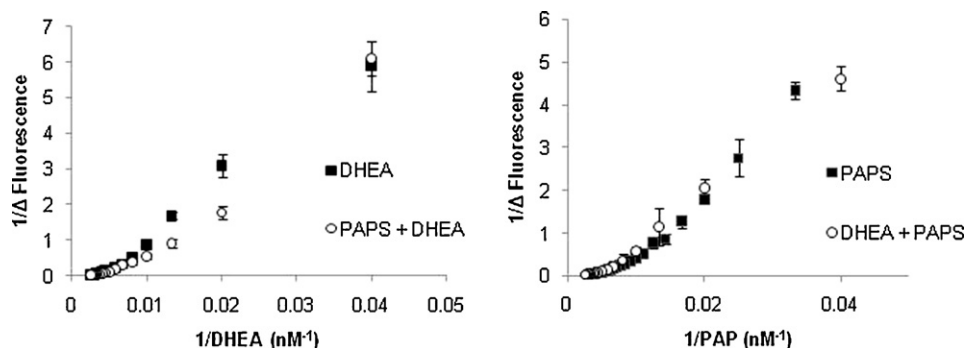


**Fig. 7.** Determination of Dissociation Constants ( $K_D$ ) of 6His-SULT2B1b-S348D. The affinity for substrates to bind to 6His-SULT2B1b was assessed using IF spectroscopy. Double-reciprocal plots expressing the change in fluorescence vs. the substrate concentration were utilized for the determination of  $K_D$ s. DHEA (A) was titrated into PBS solution containing 50 nM 6His-SULT2B1b-S348D with either no PAP or 5  $\mu$ M PAP. For B, PAP was titrated into PBS solution containing 50 nM 6His-SULT2B1b-S348D with either no DHEA or 10  $\mu$ M DHEA. PAP was used instead of PAPS to avoid in vitro sulfation of DHEA. Each experiment was performed in triplicate. Error bars represent SEM.

(Fig. 8). After 200 min, no activity was detected for 6His-SULT2B1b, while 6His-SULT2B1b-S348D retained 60% of its original sulfation activity.

### 3.8. Molecular modeling, docking studies

Since SULT2B1b-S348D is more kinetically active and robust than expressed SULT2B1b [11], studies were performed to determine whether SULT2B1b-S348D could sulfonate an increased range of putative substrates. Docking studies were initially performed to determine the ability of the putative substrates to fit into the active site of SULT2B1b constructs in a kinetically favorable conformation. In the docking studies, binding free energy (BFE) was used as a scoring function used to compare the affinity for substrates to “bind” into the active site of SULT2B1b via non-covalent interactions. 22R-hydroxycholesterol, 22S-hydroxycholesterol, 24-hydroxycholesterol and 25-hydroxycholesterol can bind SULT2B1b with BFE that are equal to or more favorable than known substrates DHEA and pregnenolone (Table 4). The BFE of binding for DHEA was  $-9.5$  kJ, pregnenolone was  $-8.9$  kJ, 22R-hydroxycholesterol was  $-10.6$  kJ, 22S-hydroxycholesterol

was  $-11.6$  kJ, 24S-hydroxycholesterol was  $-11.6$  kJ and 25-hydroxycholesterol was  $-11.4$  kJ (Table 4). For each structure, the distance between the active site histidine (H125) and the hydroxyl acceptor (3-position) of the substrate was measured to ensure that hydrogen bonding was possible. Each measurement showed distances less than 4 Å, which is conducive to hydrogen bonding (data not shown).

### 3.9. In vitro sulfation of oxysterols

Since the docking studies showed that the oxysterols could bind in kinetically favorable conformations in the active site of SULT2B1b, in vitro sulfonation assays were carried out to examine if the oxysterols were indeed substrates. Oxysterols 22R-hydroxycholesterol, 22S-hydroxycholesterol, 24S-hydroxycholesterol and 25-hydroxycholesterol were sulfated by 6His-SULT2B1b-S348D, while desmosterol and 7-dehydrocholesterol were not sulfated. As shown in Table 5, the  $K_m$  for 22R-hydroxycholesterol is  $1.0 \pm 0.01$   $\mu$ M, 22S-hydroxycholesterol is  $11.7 \pm 1.6$   $\mu$ M, 24S-hydroxycholesterol is  $9.5 \pm 0.4$   $\mu$ M, and 25-hydroxycholesterol is  $0.7 \pm 0.09$   $\mu$ M. It should be noted that 22S-hydroxycholesterol is a synthetic compound and is not a physiological oxysterol. Comparing the IF data from Table 4 and the kinetic data from Table 5, there is a general correlation between the predicted binding of substrates to SULT2B1b (BFE) and the affinity of the enzyme to sulfate the oxysterols ( $K_m$ ).

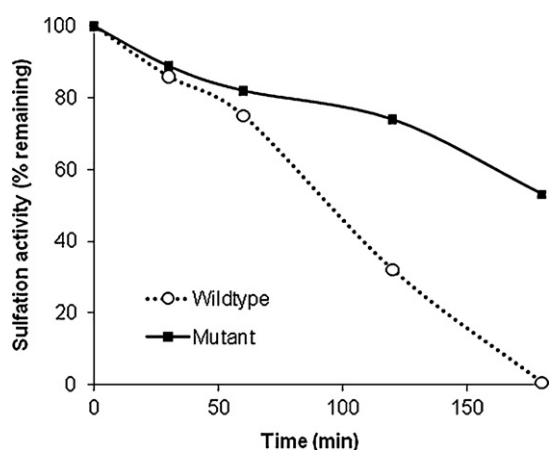


**Fig. 8.** Stability assays for SULT2B1b and SULT2B1b-S348D. The thermal stability of purified recombinant SULT2B1b and SULT2B1b-S348D was compared in a time course (A) at 42 °C and during several freeze thaw cycles (B). In each experiment, 2.5  $\mu$ g 6His-SULT2B1b or 0.25  $\mu$ g 6His-SULT2B1b-S348D was incubated with 10  $\mu$ M [ $^3$ H]-DHEA and 25  $\mu$ M PAPS for 10 min. It should also be noted that the specific activities of the SULT2B1b and SULT2B1b-S348D enzymes used in these stability assays were 10-fold different with SULT2B1b having a specific activity of 21  $\text{pmol}^{-1} \text{min}^{-1} \text{mg}^{-1}$  and SULT2B1b-S348D having a specific activity of 209  $\text{pmol}^{-1} \text{min}^{-1} \text{mg}^{-1}$ . Each reaction was performed in duplicate.

**Table 4**

Scoring values of substrates docked into SULT2B1b structures.

Substrate	Binding free energy (kJ)
DHEA	-9.6
Pregnenolone	-9.4
22R-Hydroxycholesterol	-10.6
22S-Hydroxycholesterol	-11.6
24S-Hydroxycholesterol	-11.6
25S-Hydroxycholesterol	-11.4
Desmosterol	-11.0 <sup>a</sup>
7-Dehydrocholesterol	-7.9

The molecular model for SULT2B1b S348D enzyme construct was utilized in docking experiments to determine the ability of putative substrates to access and dock into the substrate binding site for SULT2B1b. Docking experiments were performed in MOE using Proxy Triangle and Affinity dG algorithms. Binding free energy (BFE) was the scoring function used in these experiments. The top 5 ranked structures with the lowest BFE were checked for errors using NIH Structural Analysis and Verification Server (SAVES) database.

<sup>a</sup> Docking of desmosterol into SULT2B1b was not in a catalytic conformation.

**Table 5**  
Kinetic characterization of steroids and oxysterols as substrates for 6His-SULT2B1b S348D.

Substrate	$K_m$ ( $\mu\text{M}$ )	$V_{\text{max}}$ (nmol·min <sup>-1</sup> )	$K_m \cdot V_{\text{max}}^{-1}$ (min <sup>-1</sup> )
DHEA	0.9 ± 0.11	23.46 ± 0.15	3.8 × 10 <sup>-5</sup>
Pregnenolone	1.9 ± 0.07	57.68 ± 1.39	3.3 × 10 <sup>-5</sup>
22R-OHChol	1.0 ± 0.01	2.89 ± 0.02	3.5 × 10 <sup>-4</sup>
22S-OHChol (syn)	11.7 ± 1.60	26.94 ± 2.32	4.3 × 10 <sup>-4</sup>
24S-OHChol	9.5 ± 0.39	3.98 ± 0.15	2.4 × 10 <sup>-3</sup>
25S-OHChol	0.7 ± 0.09	3.70 ± 0.08	2.0 × 10 <sup>-4</sup>
7-Dehydrocholesterol	ND	ND	ND
Desmosterol	ND	ND	ND

Expressed 6His-SULT2B1b S348D enzyme was used in thin-layer chromatography assays to determine the apparent  $K_m$ s and  $V_{\text{max}}$  values for the substrates listed. Steroid and oxysterol sulfation was assayed at concentrations between 0.5  $\mu\text{M}$  and 20  $\mu\text{M}$  using 25  $\mu\text{M}$  [<sup>35</sup>S]-PAPS and 0.25  $\mu\text{g}$  enzyme. Sulfated products were detected by exposing TLC plates to autoradiography film. Sulfated bands were scraped from TLC plates and counted in liquid scintillation counter. All assays were performed in triplicate,  $K_m$  and  $V_{\text{max}}$  values are expressed as  $\pm$  SEM. ND = no sulfation activity detected.

#### 4. Discussion

Site-directed mutagenesis of SULT2B1b was initially investigated to elucidate a mechanism for nuclear localization. These experiments revealed that the phosphorylation of a single Ser residue was associated with nuclear localization of SULT2B1b. The molecular modeling and in silico mutagenesis experiments were performed to predict the effect that phosphorylation may have on SULT2B1b. Since the modeling suggested that phosphorylation might influence the structure of the enzyme, the molecular mimic SULT2B1b-S348D was expressed and purified to characterize whether “phosphorylation” affected the kinetics of the enzyme. The relatively robust sulfation activity of the purified SULT2B1b-S348D was a fortuitous observation. This increased activity suggests that the phosphorylation of SULT2B1b may be involved in both nuclear localization and regulation of sulfation activity, possibly via separate mechanisms. The hypothesis that phosphorylation of SULT2B1b has a regulatory role regarding sulfation activity was therefore investigated by the evaluation of kinetics and substrate binding behaviors for SULT2B1b-S348D.

The increased activity of the phospho-mimetic may represent a more physiologically relevant form of SULT2B1b. The hypothesized structural rearrangement of SULT2B1b-S348D upon phosphorylation may increase the catalytic potential of the enzyme, thus resulting in decreased  $K_m$  values for SULT2B1b-S348D. Since sulfation activity of SULT2B1b is lost upon disruption or lysis of cells or tissues, the functional consequence of phosphorylation is most likely a transient or labile modification. The addition of a phosphate to Ser348 could facilitate protein–protein interactions leading to the transport of SULT2B1b to the nucleus. Since SULT2B1b activity is detectable in both in the cytosol and in nuclei of intact cells, as well as with the recombinant phospho-mimetic SULT2B1b-S348D, it appears that phosphorylation is not an inactivation process. Further evaluation of expressed SULT2B1b-S348D would help to elucidate the role of Ser phosphorylation and the functional significance of SULT2B1b in the nucleus.

The published SULT2B1b crystal structures lack resolution of the N- and C- terminal extensions [22], most likely due to the dynamic nature of these regions. In order to evaluate the potential structural implications of these sequence extensions, homology models of full-length SULT2B1b were generated and utilized in in silico substrate docking experiments. Molecular models of SULT2B1b-phosphoSer348 and the molecular mimic SULT2B1b-S348D show a significant structural shift in the position of the C-terminal peptide extension compared to the molecular model of full length WT enzyme. It should be noted that the lack of information regarding

the true structure of the N- and C-terminal extension as well as the absence of homologous structures, limit the conclusions that can be drawn from the molecular modeling. For this reason, kinetic and biochemical analysis was performed on SULT2B1b-S348D to further validate this hypothesis.

The instability and poor activity of expressed SULT2B1b enzymes has made it difficult to perform binding studies. Since 6His-SULT2B1b-S348D is more structurally and enzymatically stable than expressed WT SULT2B1b, we were able to characterize the enzyme both kinetically and structurally. Binding behavior and dissociation constants ( $K_D$ ) were calculated for the enzyme as shown in Table 4. These values are consistent with values determined for SULT2A1 [31]. Since SULT2A1 and SULT2B1b are closely related enzymes which share structural homology and substrate specificity, comparisons are often made between these two isoforms in order to better understand their individual reaction mechanisms and physiological functions. The behavior of substrates binding to SULT2B1b is different from SULT2A1 since PAP binding to the enzyme has no effect on the binding of substrate. In SULT2A1, binding of PAP can inhibit the binding of bulky substrates such as Raloxifene [31]. This inhibition of large substrates binding to the enzyme in the presence of PAPS is thought to be attributed to a structural shift in the D-loop (or loop 3) in SULT2A1 [31]. Unlike SULT2A1, SULT2B1b does not show differences in binding of DHEA or pregnenolone with PAP or PAPS binding. The differences in these substrate binding behaviors suggest that SULT2B1b may utilize a different mechanism than SULT2A1 to accommodate PAPS and substrate binding.

Kinetic analysis of 6His-SULT2B1b-S348D revealed that 6His-SULT2B1b-S348D is 10-fold more active than 6His-SULT2B1b and is more stable in stability and freeze-thaw assays. It should also be noted that the addition of an N-terminal 6His-tag increases the stability of the WT expressed enzyme [11]. Removal of the 6His-tag from SULT2B1b results in a rapid loss of activity. When the 6His-tag was removed from SULT2B1b S348D, sulfation activity was retained (data not shown). The sulfation profile of various substrates has been characterized and results in  $K_m$  values up to 10 times lower than previously reported  $K_m$  values for substrates such as DHEA and pregnenolone. Similar to the C-terminal extension, the N-terminal peptide extension appears to be quite flexible and in close proximity to the substrate binding pocket, it is hypothesized that under in vitro conditions, the N-terminal peptide may block the entrance to the pocket, prohibiting substrate access to the active site of SULT2B1b.

Additionally, oxysterol substrates were characterized in a range of concentrations that are equivalent to physiological concentrations of oxysterols in circulation and in tissues such as liver and brain. Since SULT2A1 expressed is primarily localized to liver and adrenal gland, SULT2B1b is most likely responsible for the sulfation of oxysterols in extrahepatic tissues. The affinity of SULT2B1b for 22R-hydroxycholesterol and 24S-hydroxycholesterol was higher than that of previously known substrates DHEA and pregnenolone, and similar to the  $K_m$  for cholesterol (1.1  $\mu\text{M}$ ) [32]. Oxysterols are natural ligands for liver-x-receptor (LXR) which is an important transcription factor for normal physiology as it is a regulator of cholesterol, glucose and fatty acid transport and metabolism [33–37]. SULT2B1b has been shown to be regulated by nuclear receptors, such as Liver-X-Receptor (LXR), Retinoic acid-X-Receptor (RXR), and peroxisome proliferator–activator receptor (PPAR) in a variety of tissues and cell types. In human cultured keratinocytes, PPAR and LXR-activation resulted in increased SULT2B1b mRNA expression [38,39]. SULT2B1b has also been shown to affect LXR activation. Recently, the oxysterol 24S-hydroxycholesterol-3-sulfate was shown to inhibit LXR activation by blocking co-activator recruitment [40]. Overexpression of SULT2B1b in murine

dendritic cells decreased tumor growth [41]. Additionally, Bai et al. [39] demonstrated that 25-hydroxycholesterol sulfate prevented LXR-activation in human aortic endothelial cells, which lead to decreased cellular lipid levels. For these reasons, the role of oxysterol sulfation by SULT2B1b in extrahepatic tissues should be further pursued. The predicted structural rearrangement and increased sulfation activity of SULT2B1b-S348D suggest that this molecular mimic could represent a more physiologically relevant in vitro model for the study of SULT2B1b.

## References

- [1] C.N. Falany, Sulfation and sulfotransferases, introduction: changing view of sulfation and the cytosolic sulfotransferases, *FASEB J.* 11 (1997) 1–2.
- [2] T.W. Wilborn, K.A. Comer, T.P. Dooley, I.M. Reardon, R.L. Heinrichson, C.N. Falany, Sequence analysis and expression of the cDNA for the phenol-sulfating form of human liver phenol sulfotransferase, *Mol. Pharmacol.* 43 (1993) 70–77.
- [3] T. Nishiyama, K. Ogura, H. Nakano, T. Kaku, E. Takahashi, Y. Ohkubo, K. Sekine, A. Hiratsuka, S. Kadota, T. Watabe, Sulfation of environmental estrogens by cytosolic human sulfotransferases, *Drug. Metab. Pharmacokinet.* 17 (2002) 221–228.
- [4] S. Yasuda, M.Y. Liu, M. Suiko, Y. Sakakibara, M.C. Liu, Hydroxylated serotonin and dopamine as substrates and inhibitors for human cytosolic SULT1A3, *J. Neurochem.* (2007).
- [5] A. Radominska, K.A. Comer, P. Zimniak, J. Falany, M. Iscan, C.N. Falany, Human liver steroid sulphotransferase sulphates bile acids B, *Biochem. J.* 272 (1990) 597–604.
- [6] C.N. Falany, J. Wheeler, T.S. Oh, J.L. Falany, Steroid sulfation by expressed human cytosolic sulfotransferases, *J. Steroid Biochem. Mol. Biol.* 48 (1994) 369–375.
- [7] C.N. Falany, K.A. Comer, T.P. Dooley, H. Glatt, Human dehydroepiandrosterone sulfotransferase, Purification, molecular cloning, and characterization, *Ann. N. Y. Acad. Sci.* 774 (1995) 59–72.
- [8] S. Yasuda, M. Suiko, M.C. Liu, Oral contraceptives as substrates and inhibitors for human cytosolic SULTs, *J. Biochem.* 137 (2005) 401–406.
- [9] C.N. Falany, X. Xie, J. Wang, J. Ferrer, J.L. Falany, Molecular cloning and expression of novel sulphotransferase-like cDNAs from human and rat brain, *Biochem. J.* 3 (346 Pt) (2000) 857–864.
- [10] J. Lindsay, L.L. Wang, Y. Li, S.F. Zhou, Structure, function and polymorphism of human cytosolic sulfotransferases, *Curr. Drug Metab.* 9 (2008) 99–105.
- [11] C.A. Meloche, C.N. Falany, Expression and characterization of the human 3 beta-hydroxysteroid sulfotransferases (SULT2B1a and SULT2B1b), *J. Steroid Biochem. Mol. Biol.* 77 (2001) 261–269.
- [12] C. Her, T.C. Wood, E.E. Eichler, H.W. Mohrenweiser, L.S. Ramagli, M.J. Siciliano, R.M. Weinshilboum, Human hydroxysteroid sulfotransferase SULT2B1: two enzymes encoded by a single chromosome 19 gene, *Genomics* 53 (1998) 284–295.
- [13] K.A. Comer, C.N. Falany, Immunological characterization of dehydroepiandrosterone sulfotransferase from human liver and adrenal, *Mol. Pharmacol.* 41 (1992) 645–651.
- [14] N.B. Javitt, Y.C. Lee, C. Shimizu, H. Fuda, C.A. Strott, Cholesterol and hydroxycholesterol sulfotransferases: identification, distinction from dehydroepiandrosterone sulfotransferase, and differential tissue expression, *Endocrinology* 142 (2001) 2978–2984.
- [15] W.J. Geese, R.B. Raftogianis, Biochemical characterization and tissue distribution of human SULT2B1, *Biochem. Biophys. Res. Commun.* 288 (2001) 280–289.
- [16] D. He, C.A. Meloche, N.A. Dumas, A.R. Frost, C.N. Falany, Different subcellular localization of sulphotransferase 2B1b in human placenta and prostate, *Biochem. J.* 379 (2004) 533–540.
- [17] C.N. Falany, D. He, N. Dumas, A.R. Frost, J.L. Falany, Human cytosolic sulfotransferase 2B1: isoform expression, tissue specificity and subcellular localization, *J. Steroid Biochem. Mol. Biol.* 102 (2006) 214–221.
- [18] C.A. Meloche, V. Sharma, S. Swedmark, P. Andersson, C.N. Falany, Sulfation of budesonide by human cytosolic sulfotransferase, dehydroepiandrosterone-sulfotransferase (DHEA-ST), *Drug Metab. Dispos.* 30 (2002) 582–585.
- [19] D. He, C.N. Falany, Characterization of proline-serine-rich carboxyl terminus in human sulfotransferase 2B1b: immunogenicity, subcellular localization, kinetic properties, and phosphorylation, *Drug Metab. Dispos.* 34 (2006) 1749–1755.
- [20] D. He, A.R. Frost, C.N. Falany, Identification and immunohistochemical localization of sulfotransferase 2B1b (SULT2B1b) in human lung, *Biochim. Biophys. Acta* 1724 (2005) 119–126.
- [21] N.A. Dumas, D. He, A.R. Frost, C.N. Falany, Sulfotransferase 2B1b in human breast: differences in subcellular localization in African American and Caucasian women, *J. Steroid Biochem. Mol. Biol.* 111 (2008) 171–177.
- [22] K.A. Lee, H. Fuda, Y.C. Lee, M. Negishi, C.A. Strott, L.C. Pedersen, Crystal structure of human cholesterol sulfotransferase (SULT2B1b) in the presence of pregnenolone and 3'-phosphoadenosine 5'-phosphate, Rationale for specificity differences between prototypical SULT2A1 and the SULT2BG1 isoforms, *J. Biol. Chem.* 278 (2003) 44593–44599.
- [23] H. Fuda, Y.C. Lee, C. Shimizu, N.B. Javitt, C.A. Strott, Mutational analysis of human hydroxysteroid sulfotransferase SULT2B1 isoforms reveals that exon 1B of the SULT2B1 gene produces cholesterol sulfotransferase, whereas exon 1A yields pregnenolone sulfotransferase, *J. Biol. Chem.* 277 (2002) 36161–36166.
- [24] K. Lichti-Kaiser, D. Brobst, C. Xu, J.L. Staudinger, A systematic analysis of predicted phosphorylation sites within the human pregnane X receptor protein, *J. Pharmacol. Exp. Ther.* 331 (2009) 65–76.
- [25] T.B. Deramautd, D. Dujardin, A. Hamadi, F. Noulet, K. Kolli, J. De Mey, K. Takeda, P. Rondé, FAK phosphorylation at Tyr925 regulates crosstalk between focal adhesion turnover and cell protrusion, *Mol. Biol. Cell.* 22 (2011) 964–975.
- [26] N.P. Shanware, J.A. Hutchinson, S.H. Kim, L. Zhan, M.J. Bowler, Tibbetts RS, Casein kinase 1-dependent phosphorylation of familial advanced sleep phase syndrome-associated residues controls period 2 stability, *J. Biol. Chem.* 286 (2011) 12766–12774.
- [27] J.U. Bowie, R. Lüthy, D. Eisenberg, A method to identify protein sequences that fold into a known three-dimensional structure, *Science* 253 (1991) 164–170.
- [28] R. Lüthy, J.U. Bowie, D. Eisenberg, Assessment of protein models with three-dimensional profiles, *Nature* 356 (1992) 83–85.
- [29] R. Laskowski, M. MacArthur, D. Mos, J. Thornton, PROCHECK – a program to check the stereochemical quality of protein structures, *J. Appl. Crystallogr.* 26 (1993) 283–291.
- [30] C.N. Falany, T.W. Wilborn, Biochemistry of cytosolic sulfotransferases involved in bioactivation, *Adv. Pharmacol.* 27 (1994) 301–329.
- [31] I.T. Cook, T. Leyh, S.A. Kadlubar, C.N. Falany, Structural rearrangement of SULT2A1: effects on dehydroepiandrosterone and raloxifene sulfation, *Horm. Mol. Biol. Clin. Invest.* 1 (2010) 81–87.
- [32] H. Fuda, N.B. Javitt, K. Mitamura, S. Ikegawa, C.A. Strott, Oxysterols are substrates for cholesterol sulfotransferase, *J. Lipid Res.* 48 (2007) 1343–1352.
- [33] K.D. Whitney, M.A. Watson, J.L. Collins, W.G. Benson, T.M. Stone, M.J. Numerick, T.K. Tippin, J.G. Wilson, D.A. Winegar, S.A. Kliewer, Regulation of cholesterol homeostasis by the liver X receptors in the central nervous system, *Mol. Endocrinol.* 16 (2002) 1378–1385.
- [34] Y. Liang, S. Lin, T.P. Beyer, Y. Zhang, X. Wu, K.R. Bales, R.B. DeMattos, P.C. May, S.D. Li, X.C. Jiang, P.I. Eacho, G. Cao, S.M. Paul, A liver X receptor and retinoid X receptor heterodimer mediates apolipoprotein E expression, secretion and cholesterol homeostasis in astrocytes, *J. Neurochem.* 88 (2004) 623–634.
- [35] G. Cao, K.R. Bales, R.B. DeMattos, S.M. Paul, X. Liver, receptor-mediated gene regulation and cholesterol homeostasis in brain: relevance to Alzheimer's disease therapeutics, *Curr. Alzheimer Res.* 4 (2007) 179–184.
- [36] C.X. Zhang-Gandhi, P.D. Drew, Liver X receptor and retinoid X receptor agonists inhibit inflammatory responses of microglia and astrocytes, *J. Neuroimmunol.* 183 (2007) 50–59.
- [37] S. Matsumoto, K. Hashimoto, M. Yamada, T. Satoh, J. Hirato, M. Mori, X. Liver, receptor-alpha regulates proopiomelanocortin (POMC) gene transcription in the pituitary, *Mol. Endocrinol.* 23 (2009) 47–60.
- [38] Y.J. Jiang, P. Kim, P.M. Elias, K.R. Feingold, LXR and PPAR activators stimulate cholesterol sulfotransferase type 2 isoform 1b in human keratinocytes, *J. Lipid Res.* 46 (2005) 2657–2666.
- [39] Q. Bai, L. Xu, G. Kakiyama, M.A. Runge-Morris, P.B. Hylemon, L. Yin, W.M. Pandak, S. Ren, Sulfation of 25-hydroxycholesterol by SULT2B1b decreases cellular lipids via the LXR/SREBP-1c signaling pathway in human aortic endothelial cells, *Atherosclerosis* 214 (2011) 350–356.
- [40] I.T. Cook, Z. Duniec-Dmuchowski, T.A. Kocarek, M. Runge-Morris, C.N. Falany, 24-hydroxycholesterol sulfation by human cytosolic sulfotransferases: formation of monosulfates and disulfates, molecular modeling, sulfatase sensitivity, and inhibition of liver x receptor activation, *Drug Metab. Dispos.* 37 (2009) 2069–2078.
- [41] E.J. Villablanca, L. Raccosta, D. Zhou, R. Fontana, D. Maggioni, A. Negro, F. Sanvito, M. Ponzoni, B. Valentini, M. Bregni, A. Prinetti, K.R. Steffensen, S. Sonnino, J.A. Gustafsson, C. Dogliani, C. Bordignon, C. Traversari, V. Russo, Tumor-mediated liver X receptor-alpha activation inhibits CC chemokine receptor-7 expression on dendritic cells and dampens antitumor responses, *Nat. Med.* 16 (2010) 98–105.